PCCP

Accepted Manuscript

This is an *Accepted Manuscript*, which has been through the Royal Society of Chemistry peer review process and has been accepted for publication.

Accepted Manuscripts are published online shortly after acceptance, before technical editing, formatting and proof reading. Using this free service, authors can make their results available to the community, in citable form, before we publish the edited article. We will replace this *Accepted Manuscript* with the edited and formatted *Advance Article* as soon as it is available.

You can find more information about *Accepted Manuscripts* in the **Information for Authors**.

Please note that technical editing may introduce minor changes to the text and/or graphics, which may alter content. The journal's standard **Terms & Conditions** and the **Ethical guidelines** still apply. In no event shall the Royal Society of Chemistry be held responsible for any errors or omissions in this *Accepted Manuscript* or any consequences arising from the use of any information it contains.

Journal Name

ARTICLE TYPE

Aggregation of binary colloidal suspensions on attractive walls

Aleena Laganapan,[a,b] Davide Bochicchio,[b] Marguerite Bienia,[a] Arnaud Videcoq,[a] and Riccardo Ferrando[c†]

The adsorption of colloidal particles from a suspension on a solid surface is of fundamental importance to many physical and biological systems. In this work, Brownian Dynamics simulations are performed to study the aggregation in a suspension of oppositely charged colloidal particles in the presence of an attractive wall. For sufficiently strong attractions, the wall alters the microstructure of the aggregates so that B2 (CsCl-type) structures are more likely obtained instead of B1 (NaCl-type) structures. The probability of forming either B1 or B2 crystallites depends also on the inverse interaction range κa. Suspensions with small κa are more likely to form B2 crystals than suspensions with larger κa, even if the energetic stability of the B2 phase decreases with decreasing κa. The mechanisms underlying this aggregation and crystallization behaviour are analyzed in detail.

1 Introduction

Scientific investigations aimed towards the control and manipulation of colloidal structures have always attracted researchers in biomedicine and ceramics.[1–3] In itself, the study of the aggregation of colloids in suspension has greatly contributed to the advancements of colloidal science,[4,5] and is now a very active research field.[6–9] However, structural design is not entirely restricted to the self-assembly of colloids due to their mutual interactions. In fact, a powerful and more flexible way to control spatial ordering in the aggregates is by the introduction of external forces, which can bring forth new possibilities for different microstructural formations.[10–12] In this work, the external force is due to an attractive wall.

In recent years, particular attention has been given to the numerical modeling of the aggregation of colloids.[13,14] One reason is because colloids display the same phase behavior as atoms and molecules, but with the mesoscopic size advantage thus allowing direct observation in real space.[15,16] Another reason is because colloids serve as excellent models in the understanding of protein adsorption on surfaces since both systems are subject to the same thermodynamics, but with the colloids having the benefit of simpler length scales.[17,18]

In this paper, we used binary colloidal suspensions i.e. systems consisting of two types of particles, which can acquire opposite charges in the suspension and interact mainly through screened electrostatic forces. Binary systems have been prominently featured in the recent years due to the heteroaggregation phenomena[19] that can lead to even more diverse types of colloidal crystals.[11,14,20] The system used is similar to the one presented by Bochicchio et al.,[21,22] where the aggregation kinetics of binary colloidal crystallites in absence of external force fields is modeled. In Ref. 21 it has been found that the most stable colloidal crystallite structure depends on the parameter κa, in which κ is the Debye inverse length and a is the colloid radius. The obtained crystallite structures can be classified into type B1 (NaCl crystal structure) or B2 (CsCl structure) (see Fig. 1). For $\kappa a < 2.55$ (long interaction ranges) the B1 structure is energetically favored, while for $\kappa a > 2.55$ the B2 structure prevails.[14] However, the aggregation simulations show that the B1 structure is also formed for κa in the interval $2.55 - 3.3$ due to kinetic effects.[21] The study

[a] SPCTS, UMR 7315, ENSCI, CNRS, Centre Européen de la Céramique, 12 rue Atlantis, 87068 Limoges cedex, France
[b] Dipartimento di Fisica, via Dodecaneso 33, 16146, Genova, Italy
[c] Dipartimento di Chimica e Chimica Industriale and CNR-IMEM, via Dodecaneso 31, 16146, Genova, Italy
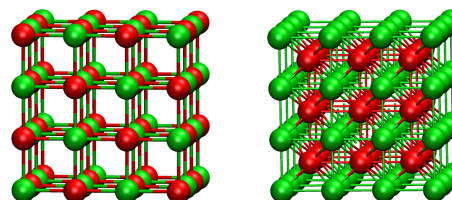‡ Corresponding author: ferrando@fisica.unige.it

Fig. 1 A B1-type lattice (left) and a B2-type lattice (right). For the B1 structure, an atom is surrounded by 6 first nearest neighbors of a different kind. For the B2 structure, an atom is surrounded by 8 first nearest neighbors of a different kind.

of the aggregation mechanism has shown that a metastable liquid aggregate is formed first. Solidification occurs when stable nuclei are formed inside this aggregate. If the $\kappa a < 3.3$, the interaction range is sufficiently large to hinder the formation of B2 nuclei, in which a particle of a given type has to be surrounded by 8 particles of the opposite charge (see Fig. 1). A subsequent metadynamics study by Bochicchio et al.[22] has shown that the transition from the metastable B1 aggregates formed for $2.55 < \kappa a < 3.3$ to the energetically stable B2 structures requires surmounting large energy barriers, so that the metastable B1 aggregates may have a very long lifetime.

The goal of this paper is to determine further possible alterations to the same binary system when an attractive wall is introduced. In light of the observation described above, we are interested in the modifications in the region where $\kappa a < 3.3$. We study the assembly of colloids on the surface and determine the parameters that affect the conformation of the colloids. In the present paper, these include the bulk parameters of the suspension (potential well depth U^* and inverse range of interaction κa), and the interaction strength between the wall and the colloids ε^*.

We perform Brownian Dynamics simulations of a binary suspension, interacting via a Yukawa potential. While it is feasible to work on realistic potentials for the colloid-wall interactions, it entails a significant slowing down of the calculations. Here, we are only interested on the general character of the binary system with attractive walls, so that this type of external force is modeled using Lennard Jones (LJ) 9-3 potential, whose well depth and range of attraction can be easily tuned. Whether the study is on colloidal adsorption[17,23,24] or protein implants,[25,26] a predictive model that is based on the properties of the colloids and surfaces is generally informative prior to experimental studies.

Our results will show that, if the interaction with the wall is sufficiently strong, there is a clear driving force towards the formation of the B2 phase. Rather counterintuitively, the wall kinetically triggers the formation of this phase more and more easily as the phase itself becomes less and less favourable from the energetic point of view.

2 Methodology

The colloidal binary system is similar to that studied in Ref. 21. An equal number for each type of colloids ($N_A = N_B = 250$) is used. The total number of colloids used in the simulations is $N_c = 500$. Both particle types have the same radius a and carry charge of the same magnitude but with opposite signs. The interaction between the particles is described by a Yukawa potential of the form:

$$U_{ij}^Y = U_0 \, \mathrm{sgn}(q_i q_j) \frac{2a}{r_{ij}} e^{-\kappa(r_{ij}-2a)} \qquad (1)$$

where U_0 is a constant that gives the value of the potential at contact, r_{ij} is the center to center distance between particles i and j, and $\mathrm{sgn}(q_i q_j)$ is the sign of the product of charges q_i and q_j. The sign of the charge on a colloid depends on the colloid being either of type A or B. In this paper, well depth values of $U^* = U_0/k_B T = 7$ and 9 are used. For the inverse interaction range κa, the following values, namely $3, 2.55, 1.5$ and 1, are tested against the attraction strength of the wall. We note that this expression for the potential
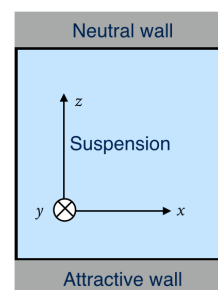

Fig. 2 Schematic diagram of the walled system. The attractive wall with varying well depth is place at $z = 0$ and a purely repulsive wall is placed at $z = L$ to avoid particles from reaching heights that are too far from the attractive wall.

is valid for $r \geq 2a$. For $r < 2a$, a hard-wall repulsion is approximated using

$$U_{ij}^{HW} = \left(\frac{r_{ij} - 2B_{ij}a}{C_{ij}} \right)^4 - D_{ij}, \qquad (2)$$

where D_{ij} has unit of an energy and regulates the depth of the well. On the other hand, the parameters B_{ij} and C_{ij} are dimensionless parameters that can be chosen such that:

$$B_{ij} = \frac{1}{2a} \left\{ r' - 4 \left[\frac{U_{ij}^Y(r) + D_{ij}}{dU_{ij}^Y(r)/dr} \right] \right\} \qquad (3)$$

$$C_{ij} = 4 \frac{[U_{ij}^Y(r) + D_{ij}]^{3/4}}{dU_{ij}^Y(r)/dr} \qquad (4)$$

where r' is the point of connection . Another alternative is to use a linear function that directly cuts the Yukawa potential at a desired distance. However, the advantage of Eq. (2) over the linear function is that the potential and the force are continuous at r'.

The interaction between the colloids and the wall is defined by an LJ 9-3 potential of the form[27]

$$U^{\mathrm{wall}}(z) = \varepsilon \left[\frac{2}{5} \left(\frac{\sigma}{z} \right)^9 - \left(\frac{\sigma}{z} \right)^3 \right], \qquad (5)$$

where ε modulates the attraction strength of the wall, $\sigma = 4a$ and z is the vertical distance from the surface of the wall. The equilibrium distance between the wall and the colloids in the suspension is $z_{\min} = 3.1a$. We note that $\sigma = 1.2a$ is also tested and similar results to $\sigma = 4a$ are obtained. Similar to Eq. (1), $\varepsilon^* = \varepsilon/k_B T$ when expressed in dimensionless units.

The suspensions are relatively dilute with volume fraction of $\phi = 0.2$. In the present paper, we assume that the hydrodynamic interactions are significantly small. A purely repulsive wall is also placed at $z = L$ to limit the freedom of the colloids along the z direction. Our system is periodic along x and y directions. A schematic diagram is shown in Fig. 2.

We choose the time unit as $t^* = 4a^2/D_0$, where D_0 is the diffusion coefficient of isolated colloids in the suspension.[21] Hence t^* is the time taken by an isolated colloid to diffuse across a distance equivalent to its diameter. The Langevin equation is solved by using a time step of $4 \times 10^{-7} t^*$ and the numerical calculations

are performed by employing the Brownian Dynamics algorithm of GROMACS.[28]

3 Parameters for aggregate analysis

P_2 is a parameter used to discriminate the formation of B1 or B2 structures.[21,22] This is defined as follows:

$$P_2 = \frac{1}{N_c} \sum_{i \neq j} \left[\frac{1}{12} e^{-\frac{(r_{ij} - r_{B1})^2}{2\sigma_{B1}^2}} - \frac{1}{6} e^{-\frac{(r_{ij} - r_{B2})^2}{2\sigma_{B2}^2}} \right], \quad (6)$$

where the sum is restricted to pairs i, j of the same type. In P_2, the different equilibrium distances of second neighbors in the B1 and B2 lattice are used to discriminate between them. The first term of the sum in P_2 counts how many neighbors a colloid of a given type has around a distance $r_{B1} = 2.98a$, which is the distance of second neighbors in the B1 lattice. The second term counts how many neighbors there are around a distance $r_{B2} = 2.46a$, which is the distance of second neighbors in the B2 lattice. The values of r_{B1}, r_{B2} and their corresponding standard deviations $\sigma_{B1} = \sigma_{B2} = 0.097a$ are obtained from the radial distribution function of the colloids.

As a further verification step, a two-dimensional version of Eq. (6) is used. It was observed that the first layers of B1 and B2 structures attached to the surface of the wall can be differentiated. A B1 structure will have its (100) plane attached to the surface wall while a B2 structure will have its (101) plane attached to the surface of the wall. The (100) B1-plane leads to a square lattice with one side having r_{B1} while the (101) B2-plane leads to a rectangular lattice with r_{B2}. In 2D, the number of second nearest neighbors (SNN) for B1 with r_{B1} is 4; while the SNN for B2 with r_{B2} is 2. Taking this into consideration, the parameter P_3 is defined as follows:

$$P_3 = \frac{1}{N_s} \sum_{i \neq j} \left[\frac{1}{4} e^{-\frac{(r_{ij} - r_{B1})^2}{2\sigma_{B1}^2}} - \frac{1}{2} e^{-\frac{(r_{ij} - r_{B2})^2}{2\sigma_{B2}^2}} \right], \quad (7)$$

where N_s is the total number of colloids in the first layer ($3.1a < z < 3.5a$).

4 Results

4.1 Strength of the wall (ε^*) vs. colloid-colloid interaction (U^*)

First, we illustrate the effect of the wall on a suspension. We use a system with $U^* = 9$ and $\kappa a = 2.55$ as an example. In the system without the wall, the expected final structure of aggregates is B1.[21] Fig. 3 shows what happens to the suspension when a wall with $\varepsilon^* = 10$ is introduced. In the initial stages of the simulation ($t = 2.5t^*$), B1-type seeds are observed outside the attraction range of the wall ($z = 10.7a$). However, towards the end of the simulation, when all of the colloids are attached to the aggregate grown on the surface, the B1-type seeds disappear and only B2 structures are left. This means that the wall can alter the colloidal structure by forming B2-type lattices instead of metastable B1-type lattices. To measure the extent of this effect, the strength of the colloid-wall interaction (ε^*) is varied.
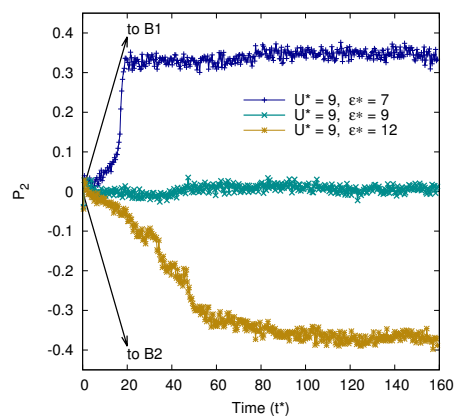
Fig. 4 shows a sample P_2 measurement when ε^* is varied to

Fig. 4 Different structures formed on the wall with varying ε^*. The suspensions used have $\kappa a = 2.55$ and $U^* = 9$.

Table 1 Different structures formed on the wall with varying ε^* for suspensions with $U^* = 9$ and 7 respectively

$U^* = 9$ $\kappa a = 2.55$				$U^* = 7$ $\kappa a = 3$			
ε^*	B1	B2	Mixed	ε^*	B1	B2	Mixed
7	3	0	2	5	4	1	0
8	2	1	5	6	2	2	1
9	3	2	3	7	3	1	1
10	1	1	3	8	1	3	1
12	0	5	0	9	1	3	1
15	0	3	2	10	2	3	0

7, 9 and 12 while keeping U^* constant at 9. A positive P_2 corresponds to a structure with dominant B1-type lattices while a negative P_2 corresponds to a structure with dominant B2-type lattices. For $P_2 < |0.05|$, the structure is considered either as a mixture of both lattice types or remains disordered. It appears from Fig. 4 that the transformation from B1 to B2 occurs when $\varepsilon^* > U^*$. To check this observation, the range of ε^* is widened and 5-8 simulations are performed for suspensions with $U^* = 9, \kappa a = 2.55$ and $U^* = 7, \kappa a = 3$. The final structures are tabulated in Table 1. The results confirm that there is a higher probability of obtaining B2 structures when $\varepsilon^* > U^*$. On the other hand, when $\varepsilon^* < U^*$, the structures tend to remain of the B1 type.

4.2 Strength of the wall (ε^*) vs. inverse range of interaction (κa)

To see if the inverse range of interaction can also affect the structure of the colloids, an additional system with $\kappa a = 1.5$ is tested against the system with $\kappa a = 2.55$, where both systems have $U^* = 9$. The results are presented in Table 2.

First, we observe a similar trend for both κa, i.e. the formation of B2 structures is more likely when $\varepsilon^* > U^*$. However, the probability of obtaining B2 structures is even higher in suspensions with $\kappa a = 1.5$ than $\kappa a = 2.55$ (compare Table 2 with Table 1). This is indeed quite counterintuitive, because decreases of κa weaken the energetic stability of the B2 phase with respect to the B1 phase[14], both in the absence and in the presence of the wall.

A possible explanation for this result is the following. In the absence of the wall, aggregation in suspensions with a longer in-
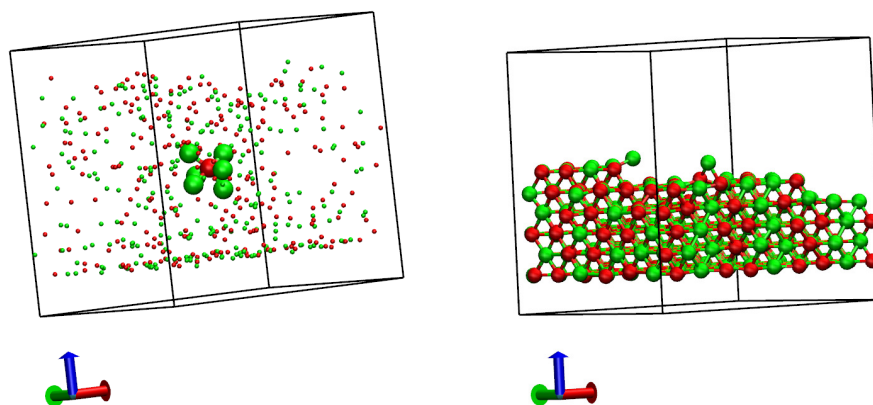
Fig. 3 Snapshots of the suspension with $U^* = 9$, $\kappa a = 2.55$ and $\varepsilon^* = 10$ at $t = 2.5t^*$ (left) and at $t = 160t^*$ (right). The radii of the colloids are scaled for clarity. In the beginning, a few B1-type seeds are formed at a distance far from the range of attraction of the wall. At the end of the simulation, only B2 structures are observed.

Table 2 Different structures formed on the wall with varying ε^*, for suspensions with $U^* = 9$ and $\kappa a = 1.5$

ε^*	$\kappa a = 1.5$		
	B1	B2	Mixed
7	1	4	0
8	2	6	0
9	2	4	2
10	0	5	0
12	0	5	0
15	0	5	0

teraction range ($\kappa a = 1.5$) is kinetically more difficult than the aggregation in suspensions with a shorter range ($\kappa a = 2.55$). Hence the role of the wall in promoting aggregation and crystallization is more important for small κa. Since crystallization at the wall is in the B2 lattice, the final results is that the formation of B2 crystallites is more likely for $\kappa a = 1.5$ than 2.55.

To further support this explanation, an interaction range of $\kappa a = 1$ with $U^* = 9$ is also tested. We have observed that only one colloidal layer can be formed on the wall surface while the remaining colloids remain in suspension. Moreover, the measured P_2 and P_3 for $\kappa a = 1$ are always negative (B2) regardless of the value of ε^* used. Therefore the systems in which aggregation is more difficult, are more susceptible to the restructuring induced by the wall.

4.3 B2-type formation starts from the wall

To establish that the formation of B2 structures is due to the nucleation occurring at the interface with the wall, the P_2 parameter is measured layer by layer. This is illustrated in Figs. 5 and 6. When the system forms a B2 structure (see Fig. 5), the layer in contact with the wall goes to negative values of P_2 first, followed then by the second layer and so on. This confirms that the nucleation starts at the interface with the wall.

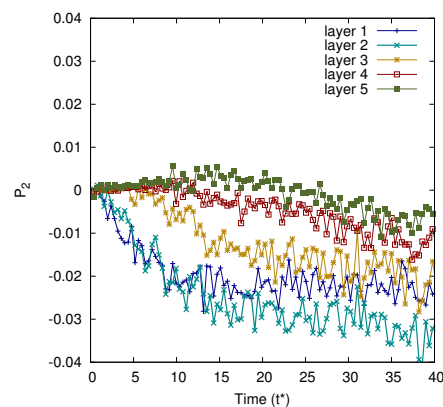On the contrary, when the system forms a B1 structure (see

Fig. 5 P_2 parameter that is measured in the beginning of the simulation for a system that forms a B2 structure.
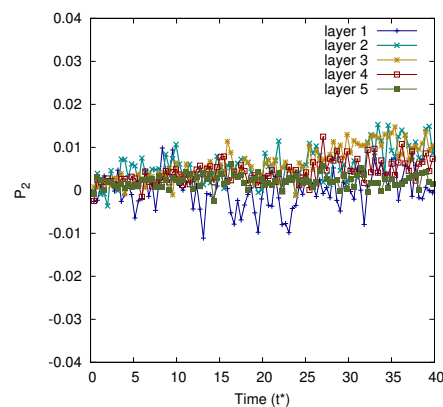

Fig. 6 P_2 parameter that is measured in the beginning of the simulation for a system that forms a B1 structure.

Fig. 6), there is no significant nucleation of B1-type seeds at the interface with the wall, since P_2 values simply become positive at the same time for all layers. This behavior is expected because the

B1-type seeds are observed to form inside the aggregates, without specific preference on z.

We can analyze this closely by looking at the process of B1 crystallite formation. For this part, we plot the B2 component of P_2. This is shown in Fig. 7. When the strength of the wall is not sufficiently high ($\varepsilon^* = 8$ vs. $U^* = 9$), the wall still attempts to form B2-type seeds in the first layers but these are eventually suppressed by the predominant B1-type seeds that form elsewhere at higher z. Towards the end of the simulation, the B2-type seeds gradually disappear and the structure becomes B1.
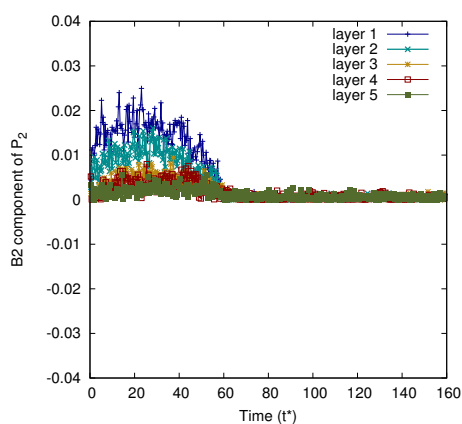
Fig. 7 B2 component of the P_2 parameter that is measured layer-by-layer for a system with $\varepsilon^* = 8$ and $U^* = 9$. The final structure is B1. It can be observed that B2-type seeds are formed on the surface of the wall but are eventually suppressed by the B1-type lattices as time progresses.

Additionally, we have observed that the arrangements of the colloids on the surface of the wall are different in the B1 and B2 cases. An example is shown in Fig. 8. To quantify the difference, the parameter P_3 for the first layer is calculated (see Fig. 9). A general trend that is present among the samples is that in the beginning of the simulation, the P_3 becomes immediately negative. When the whole aggregate crystallizes in the B2 structure, P_3 remains negative. In contrast, when the structure crystallizes as B1, the first layer rearranges and P_3 becomes positive.
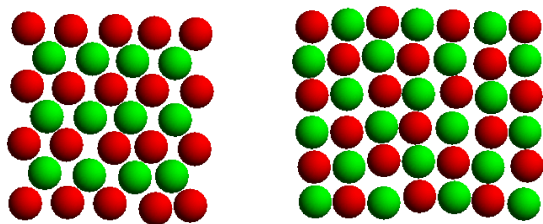

Fig. 8 The arrangement of first layer of colloids at the surface of the wall. The B2 structure (left) has its (101) plane attached at the surface of the wall while the B1 structure (right) has its (100) plane attached at the surface of the wall. The two kinds of arrangements lead to P_3 values of different signs.
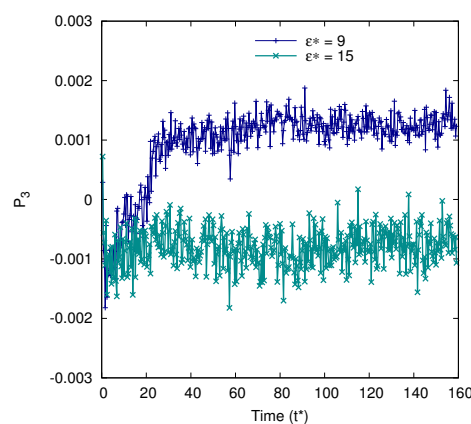

Fig. 9 P_3 parameter for the system with $U^* = 9$ and $\kappa a = 1.5$. The system with $\varepsilon^* = 9$ becomes B1 while the system with $\varepsilon^* = 15$ becomes B2.

4.4 Number of colloids per layer and interaction energy with the wall

Now that we have established that the B2-type nucleation starts in the vicinity of the wall, the next step is to understand why this type of formation occurs. To answer this, the following parameters are checked for both structures: (1) the number of colloids packed in the first layer and (2) the total interaction energy between the colloids and the wall.

Fig. 10 shows the number of colloids that can be found at certain distance from the wall at the end of the simulation ($t = 160t^*$). The peaks of the histogram correspond to each of the planes parallel to the surface of the wall. From the figure, it can be discerned that the number of colloids packed in the first layer is significantly larger in the B2-type case. In the system used in Fig. 10, there are 81 and 94 colloids on the surface of the wall ($3.1 < z/a < 3.4$) for the B1 and B2 structures respectively. This trend is generally observed in all of the samples. Moreover, the distances between the peaks are smaller for the B2 case suggesting a more compact and favorable ordering.

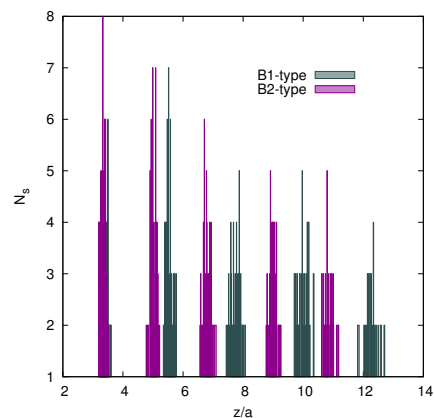Next, we compare the total interaction energy between the col-

Fig. 10 Sample number of colloids vs. the distance from the wall ($U^* = 9$, $\kappa a = 1.5$ and $\varepsilon^* = 8$). The peaks correspond to the planes of colloids that are parallel to the surface of the wall.
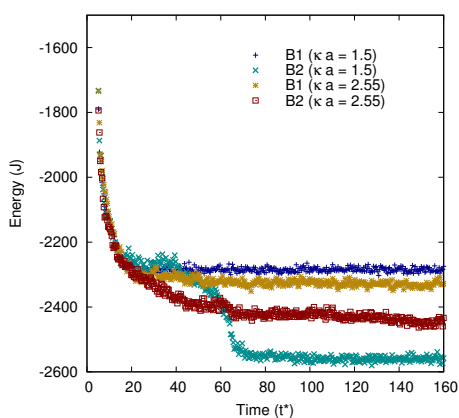
Fig. 11 Comparing the colloid-wall interaction energies for B1 vs. B2 structures. We compare $\kappa = 1.5$ and 2.55 for systems with $U^* = 9$ and $\varepsilon^* = 8$.

loids and the wall using a suspension with $U^* = 9$, $\kappa a = 1.5$ and $\kappa a = 2.55$. This is shown in Fig. 11. For both systems, the simulations that yield B2 structures have lower energies than the simulations that yield B1 structures.

Finally, we confirm that the B2 transformation is not induced by finite size effects. P_2 is measured for different box lengths L and system size N_c, while keeping the volume fraction constant. The values of L used are $22a, 22.5a, 22.75a, 23a, 24a, 25a$ and $26a$. The results in Fig. 12 show that B2 structures are always obtained, independently on the system size.
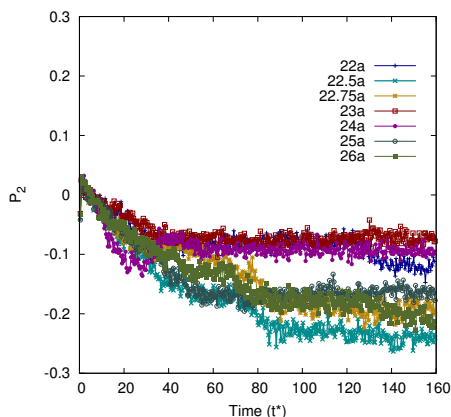

Fig. 12 The influence of L on the parameter P_2 for systems with $U^* = 9$, $\kappa a = 1.5$ and $\varepsilon^* = 15$. The results prove that the formation of B2 structures is not induced by finite size effects.

5 Conclusions

In conclusion, we have demonstrated by means of Brownian Dynamics simulations that introducing an attractive wall in a binary system of colloids, alters the probability of forming different types of colloidal crystals. This happens for a wall which is perfectly flat and homogeneous, which may be thought as not introducing any bias in favour of any specific interface. Our results show that this is not the case, because the flat homogeneous wall favours the formation of a specific crystal structure.

The extent of the effects induced by the wall depends on the properties of the suspension and on the strength of the attraction with the wall. Specifically, when the attraction strength of the wall exceeds the attraction strength between the colloids ($\varepsilon^* > U^*$), the probability of forming a B2 structure is higher than its B1-type counterpart. This happens not only for $2.55 \leq \kappa a \leq 3.3$, where metastable B1 aggregates are formed in the absence of the wall, but even for $\kappa a < 2.55$, where the B1 phase becomes energetically favourable for the values of $U_0/(k_B T)$ considered here. [14]

Surprisingly, we have observed that the wall causes the formation of B2 crystallites more easily in suspensions with $\kappa a = 1.5$ than in suspensions with $\kappa a = 2.55$ and $\kappa a = 3$. This is a rather counterintuitive behaviour, because the B2 phase becomes less and less energetically favourable with decreasing κa. [14] The explanation of this result derives from observing that aggregation in the absence of the wall is kinetically more difficult for small κa. Therefore, the action of the wall in promoting aggregation and crystal nucleation is even more important for such κa, thus triggering the growth of B2 aggregates.

On the other hand, when $\varepsilon^* < U^*$, the behaviour is similar to that found in the absence of the wall. [21]

Our analysis has demonstrated that B2-type seeds start forming at the interface layer with the wall and slowly build up layer by layer. B2 formation is more favorable because it allows the colloids to be more closely packed at the interface with the wall. In addition to this, we have observed that the total interaction energy between the aggregate and the wall is also lower for B2 structures than for B1 structures.

From these results, it follows that the formation of metastable (and even stable) B1 phases can be suppressed when a sufficiently strong interaction with a wall is introduced.

Finally, we note that our results can be important not only for understanding the mechanisms that rule the colloid aggregation in the presence of external force fields, but also for designing strategies to obtain colloidal crystals with the desired structures.

Acknowledgements

References

1 M. Y. Lin, H. M. Lindsay, D. A. Weitz, R. C. Ball, R. Klein and P. Meakin, *Nature*, 1989, **339**, 360–362.

2 R. Hidalgo-Álvarez, A. Martín, A. Fernández, D. Bastos, F. Martín and F. J. de las Nieves, *Adv. Colloid and Interface Sci*, 1996, **67**, 1–118.

3 R. Prasher, P. E. Phelan and P. Bhattacharya, *Nanoletters*, 2006, **6**, 1529–1534.

4   B. V. Derjaguin and L. D. Landau, *Acta Physicochim. URSS*, 1941, **14**, 63352.

5   E. . J. W. Verwey and J. T. G. Overbeek, *Theory of Stability of Lyophobic Colloids*, Elsevier, The Netherlands, 1948.

6   J. M. López-López, A. Schmitt, A. Moncho-Jordá and R. Hidalgo-Álvarez, *Soft Matter*, 2006, **2**, 1025.

7   E. Sanz, C. Valeriani, T. Vissers, A. Fortini, M. E. Leunissen, A. van Blaaderen, D. Frenkell and M. Dijkstra, *J. Phys.: Condes. Matter*, 2008, **20**, 494247.

8   M. Bier, R. van Roij and M. Diijkstra, *J. Chem. Phys.*, 2010, **133**, 124501.

9   G. Pavaskar, S. Sharma and S. N. Punnathanam, *J. Chem. Phys.*, 2012, **136**, 134506.

10 N. Vogel, M. Retsch, C. D. Fustin, A. del Campo and U. Jonas, *Chem. Rev.*, 2015, **115**, 6265–6311.

11 K. P. Velikov, C. G. Christova, R. P. A. Dullens and A. van Blaanderen, *Science*, 2002, **296**, 106–109.

12 J. J. Kim, *Langmuir*, 2011, **27**, 2334–2339.

13 J. A. Lewis, *J. Am. Ceram. Soc.*, 2000, **83**, 2341–59.

14 M. E. Leunissen, C. G. Christova, A. P. Hynninen, C. P. Royall, A. I. Campbell, A. Imhof, M. Dijkstra, R. van Roij and A. van Blaaderen, *Nature*, 2005, **437**, 235–239.

15 A. Yethiraj and A. A. van Blaaderen, *Nature*, 2003, **421**, 513–517.

16 W. K. Kegel and A. van Blaaderen, *Science*, 2000, **287**, 290–293.

17 M. R. Oberholzer, N. J. Wagner and A. M. Lenhoff, *J. Chem. Phys.*, 1997, **107**, 9157–9167.

18 M. Malmsten, *J. Colloid and Interface Sci.*, 1998, **207**, 186–199.

19 M. Cerbelaud, A. Videcoq, P. Abélard, C. Pagnoux, F. Rossignol and R. Ferrando, *Langmuir*, 2008, **24**, 3001–3008.

20 E. C. M. Vermolen, A. Kuijk, L. C. Filion, M. Hermes, J. H. J. Thijssen, M. Dijkstra and A. van Blaaderen, *Proc Natl Acad Sci U S A*, 2009, **106**, 16063–16067.

21 D. Bochicchio, A. Videcoq and R. Ferrrando, *Phys. Rev. E.*, 2013, **87**, 022304.

22 D. Bochicchio, A. Videcoq and R. Ferrrando, *J. Chem. Phys.*, 2014, **140**, 024911.

23 P. Gonźales-Mozuelos, M. Medina-Noyola, B. D'Aguanno, J. M. Méndez-Alcaraz and R. Klein, *J. Chem. Phys.*, 1991, **95**, 7461–7466.

24 H. Wang and B. Z. Newby, *Biointerfaces*, 2014, **9**, 041006.

25 M. R. Oberholzer and A. M. Lenhoff, *Langmuir*, 1999, **15**, 3905–3914.

26 J. J. Gray, *Current Opinion in Structural Biology*, 2004, **14**, 110–115.

27 J. P. Hansen and I. R. McDonald, *Theory of Simple Liquids*, Academic Press, San Diego, CA, 2nd edn, 1986.

28 D. van der Spoel, E. Lindahl, B. Hess, G. Groenhof, A. E. Mark and H. J. C. Berendsen, *J. Comput. Chem*, 2005, **26**, 1701.

29 W. Humphrey, A. Dalke and K. Schulten, *J. Mol. Graphics*, 1996, **14**, 33–38.

Physical Chemistry Chemical Physics Accepted Manuscript